Journal of Molecular Modeling (2023) 29:130
https://doi.org/10.1007/s00894-023-05535-2

ORIGINAL PAPER

In silico identification and molecular dynamic simulations of derivatives of 6,6-dimethyl-3-azabicyclo[3.1.0] hexane-2-carboxamide against main protease 3CL^{pro} of SARS-CoV-2 viral infection

Prashasti Sinha[1] · **Anil Kumar Yadav**[1]

Received: 3 December 2022 / Accepted: 28 March 2023 / Published online: 5 April 2023

Abstract

Context The unavailability of target-specific antiviral drugs for SARS-CoV-2 viral infection kindled the motivation to virtually design derivatives of 6,6-dimethyl-3-azabicyclo[3.1.0]hexane-2-carboxamide as potential antiviral inhibitors against the concerned virus. The molecular docking and molecular dynamic results revealed that the reported derivatives have a potential to act as antiviral drug against SARS-CoV-2. The reported hit compounds can be considered for in vitro and in vivo analyses.

Methods Fragment-based drug designing was used to model the derivatives. Furthermore, DFT simulations were carried out using B3LYP/6-311G** basis set. Docking simulations were performed by using a combination of empirical free energy force field with a Lamarckian genetic algorithm under AutoDock 4.2. By the application of AMBER14 force field and SPCE water model, molecular dynamic simulations and MM-PBSA were calculated for 100 ns.

Keywords Molecular docking · Boceprevir · Main protease 3CL^{pro} · Molecular dynamic

Introduction

Future decades are expected to encounter changes in climatic conditions. The changes in the climate will be due to greenhouse effect and depletion of ozone layer. By 2100, the global mean temperature of surface air is expected to increase by about 2°C. Now, as the Earth tends to get warmer, the spread of disease by mosquitoes will significantly increase. Also, the rising temperature will open the doors for melting of glaciers, thereby increasing the spread of diseases and contaminants. Therefore, the need of drugs will drastically increase and most of these drugs will be novel, since the target (disease) will be new or some variants of the existing ones.

Drug development is a costly, time-taking, and complicated process, exhibiting high rates of uncertainty for a drug to become successful. Based on our past experience of exposure to COVID-19, an ample amount of efforts were put in by the researches and scientists worldwide to synthesize a drug or a vaccine. After so many attempts, we still have not succeeded in making a drug specially designed for SARS-CoV-2 and its variants. Therefore, to increase the success rate while designing a drug compound, computer-aided drug designing (CADD) are taken into account. Amongst the different methods of CADD, fragment-based drug designing (FBDD) is one of the popular methods to design novel structures using fragment/core of the available drug compounds. The method reduces attrition and provides leads for intractable biological targets. Therefore, the goal of the work is to virtually design and screen some novel hit compounds that exhibit inhibition against SARS-CoV-2 main protease 3CL^{pro}.

Members of the Coronaviridae family, SARS-CoV-2, are prevailing globally since 2019 [1]. Severe acute respiratory syndrome induces viral respiratory disease; the viral infection emerged in the year 2002 in some parts of China [2]. The airborne virus is highly transmissible and spread via tiny droplets released from the infected patient while sneezing or coughing and or by usual respiration. Followed by the incubation duration of 2–7 days, the preliminary symptoms

✉ Anil Kumar Yadav
akyadavbbau@gmail.com

[1] Department of Physics, School of Physical & Decision Science, Babasaheb Bhimrao Ambedkar University, Lucknow 226025, Uttar Pradesh, India

observed are high fever (> 100 °F), cough, sore throat, dizziness, palpitations in the chest, and rapid reduction in white blood cells. SARS-CoV-2 has a high mortality rate wherein deaths are induced due to the alveolar damage and respiratory failure. Although after making several attempts to control the spread, still the virus affected 218 countries, infecting 620,301,709 people which includes 6,540,487 deaths around the globe (reported by WHO, 13 October 2022).

Genomic structures of SARS-CoV-2 are typified by a size of 30 kB and possess spike glycoproteins, envelop glycoprotein, nucleocapsid protein, and different non-structural proteins [3]. Ephemeral glycol proteins have receptor-binding domain (RBD) which individually recognizes ACE2 [4]. These regions are often subjected to mutations affecting the morbidity, pathophysiology, and rate of transmission of corona virus [5–8]. The primary protease present in coronaviruses is the 3C-like protease ($3CL^{pro}$) or main protease (M^{pro}), also known as C30 endopeptidase or 3-chymotrypsin-like protease. It uses eleven homologous sites to break the coronavirus polyprotein. It belongs to the PA family of cysteine proteases and is a cysteine protease. It breaks a Gln-(Ser/Ala/Gly) peptide link and has a cysteine-histidine catalytic dyad at its active site [9, 10]. In 2011, boceprevir (protease inhibitor) was approved by the FDA to cure HCV genotype 1. Lately, Lifeng Fu et al. in 2020 reported the inhibitory activity of boceprevir with main protease enzyme $3CL^{pro}$ of SARS-CoV-2 [11]. But there were some corollary effects of the drugs such as nausea, fatigue, insomnia, and many more.

Consequently, redesigning of chemical compounds of novel FBDD structures that are easy to synthesize in laboratories were computationally designed. The initial structure designing was carried out by generating active fragments and linking it to the core molecule in order to design a novel compound, resulting in the generation of new and effective hit candidates to treat main protease. Hence, the study resulted in three novel drug structures, virtually optimized to efficaciously treat COVID-19.

Methodology

The designing of the reported compound was done via ACFIS [13], and the theoretical calculations were carried out using Gaussian 09 software [14]. All the computations were performed at B3LYP/6-311G** basis set [15, 16]. Using geometry optimization, the geometries of the compounds were redefined. This step was followed by the estimation of vibrational transitions of the optimized compounds in order to authenticate that the designed compounds are not optimized at transition state but at minimum state. This was followed by the calculation of electronic, thermodynamic, and pharmacological properties of the optimized compounds, and then our computed results {Boceprevir [cal]} were compared to the experimental results {Boceprevir [ref]} of boceprevir [18, 19]. Moreover, the optimized compounds were docked to PDB ID: 7C6S known for SARS-CoV-2 main protease $3CL^{pro}$. This protein target was used for analyzing the interaction with derived hit compounds to understand the inhibitory activity with $3CL^{pro}$ using AutoDock 4.2 docking software [17]. This software combines empirical free energy force field with a Lamarckian genetic algorithm to yield better and fast conformations. The best docked complex was subjected to molecular dynamic simulation using AMBER14 force field SPCE water model at using YASARA software [21, 22]. Other calculations such as hydrogen bond analysis and MM-PBSA signify the strength and stability of the complex in the binding cavity [23].

Results and discussion

Fragment-based drug designing

The three hit compounds of the boceprevir are here referred as derivatives of 6,6-dimethyl-3-azabicyclo[3.1.0]hexane-2-carboxamide. Table 1 gives the brief description about the optimized compounds.

The initial screening resulted in various candidate generation using fragment linking via ACFIS 2.0. PDB complex of main protease of SARS-CoV with boceprevir was used to generate cores. These derived cores were transformed to potential drug candidate by linking fragments from the databases already available on the web server. Amongst several compounds, 3 candidates were identified based on their ligand efficiency score for further validation as potential drugs for inhibiting $3CL^{pro}$.

There is a great potential in probing unidentified "chemical space" to create innovative biologically active compounds with innovative and effective substrates in order to sustain ingenuity and optimize the efficacy of therapeutic revelation. As a consequence, fragment-based drug development experienced rapid growth due to the enhanced extensive investigation for "chemical space," which can contribute to an increased success probability and ligand effectiveness. PARA GEN, CORE GEN, and CAND GEN are the three computational programs featured in ACFIS web server. Employing fragment disassembly technique, ACFIS can create core fragments from the bioactive component and accomplish in simulated evaluation by expanding segments to the intersection of core structures. Fragments normally have a low affinity for respective binding sites; hence, the affinity must be

Table 1 Optimized compounds in the reported study.

Compound	Structure	Molecular Formula	Molecular Mass	IUPAC name
1.	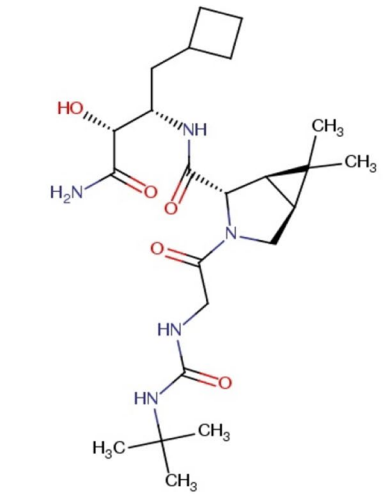	C23H39N5O5	465.29 amu	(1R, 2S, 5S)-N-(4-amino-1-cyclobutyl- 2,3-dioxobutan-2-yl)-3-[(2S)-2-(tert-butylcarbamoylamino) -ethanoyl]- 6,6- dimethyl-3- azabicyclo[3.1.0]hexane-2-carboxamide
2.	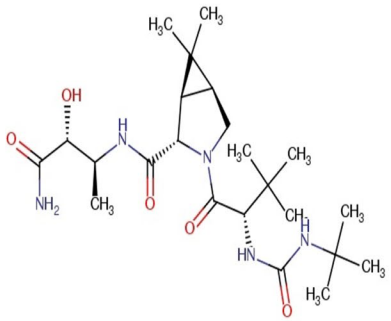	C23H41N5O5	467.31 amu	(1R, 2S, 5S)-N-(4-amino-3,4- dioxopentan-2-yl)-3- [(2S)-2-(tert-butylcarbamoylamino) -3,3-dimethylbutanoyl]-6,6-dimethyl-3-azabicyclo[3.1.0]hexane-2-carboxamide
3.	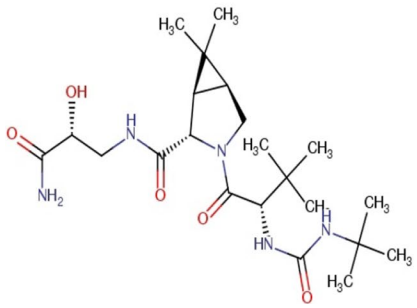	C22H39N5O5	439.31 amu	(1R, 2S, 5S)-N-(4-amino-2,3- dioxopropan-2-yl)-3- [(2S)-2-(tert-butylcarbamoylamino) -3,3-dimethylbutanoyl]-6,6-dimethyl-3-azabicyclo[3.1.0]hexane-2-carboxamide

enhanced by adding supplemental substituent or integrating two hit fragments confined in local binding pockets. Ligand efficiency is an extensively employed notion which is frequently used to test multiple hit fragments for lead creation and standardization operation.

Geometry optimization

The shortlisted molecular structures were subjected to energy and geometry optimization. Apart from thermodynamic estimations from energy and geometry minimization,

Table 2 Electronic and thermodynamic values of boceprevir and designed compounds using B3LYP/6-311G**

Compounds	Total energy (kcal/mol)	Entropy (calmol^{-1} K^{-1})	HOMO (eV)	LUMO (eV)	ΔE (eV)	Ionization potential (eV)	Dipole moment (Debye)	Heat of formation (kcal/mol)
Boceprevir (ref)	− 176,734	208.31	− 9.603	0.008	9.611	− 9.603	2.651	− 205.945
Boceprevir (cal)	− 175,213	205.27	− 9.612	0.075	9.687	− 9.711	2.974	− 206.121
1	− 235,246	173.22	− 9.322	-0.745	8.577	− 9.847	4.12	− 357.589
2	− 245,501	233.85	− 9.219	-0.658	8.561	− 9.749	2.93	− 328.214
3	− 239,875	213.82	− 9.395	-0.711	8.684	− 9.88	8.51	− 349.549

Here, boceprevir (ref) refers to the experimental data and boceprevir (cal) refers to the computationally calculated data.

there is spectroscopic calculations which were computed using the same computational package. Spectroscopic frequencies are calculated by determining the second derivatives of the energy corresponding to the Cartesian nuclear parameters and translating them to bulk variables. Only at a static site is this conversion feasible. As a corollary, using the approach employed for spectrum calculation, computing spectra at any configuration besides a fixed axis is irrelevant. Table 2 depicts the electronic and thermodynamical values after geometry optimization.

The above-stated properties involve the total energy, HOMO energy, LUMO energy, ΔE known as frontier molecular orbital energy gap, entropy, ionization potential, dipole moment, and heat of formation. With reference to Table 2, the experimental and computational energy derived in the study are nearly same, that is, − 176,734 kcal/mol, whereas the virtual designs have a varied energy range from − 245,501 kcal/mol to − 235,246 kcal/mol. This clearly indicates that designed hit compounds have lower energy as compared to FDA-approved boceprevir. Compound 2 is observed to have the lowest energy amongst all other compounds, and therefore, it is probably more stable than the other reported molecular structures. Boceprevir possesses HOMO which is − 9.6 eV, and other reported hit compounds possess HOMO in the range of − 9.2 to − 9.3 eV. It can be seen that there is no significant difference between the HOMO values of boceprevir and reported compounds. But the LUMO value of boceprevir is 0.008 eV, and for the other compounds, it ranges from − 0.745 to − 0.658 eV. Since this difference in LUMO values is large, therefore it causes difference in the values of ΔE ranging from 8.561 to 8.684 eV which is less as compared to the ΔE value of boceprevir which is reported to be 9.611 eV. This shows that the reported hit compounds possess more reactivity with the medium surrounding it than the FDA-approved boceprevir. The table shows the values for entropy of the reported compounds possesses lesser entropy in the range of 173.22 (calmol^{-1} K^{-1}) to 233.85 (calmol^{-1} K^{-1}) as compared to boceprevir (208.31 calmol^{-1} K^{-1}); the lower entropy indicates that the reported compounds are more stable. The dipole moment of the reported compounds ranges from 2.93 Debye for compound 2 to 8.51 Debye for compound 3. Therefore, in the table, compound 1 and compound 3 exhibit high dipole moments which indicate the high reactivity of the compound with the surrounding media; that is, the higher the dipole moment, the more will be the reactivity of the compound. Furthermore, the heat of formation is the change in enthalpy collateral with the generation of 1 mol of compound using the elements in their stable states having the physical conditions of 1 atmosphere pressure and any described temperature. Reported compounds possess lower heat of formation as compared to boceprevir. Thus, the reported hit compounds are more stable than the boceprevir.

Table 3 Pharmacological descriptors for boceprevir and reported optimized hit compounds

Compounds	Surface (A^2)	Volume (A^3)	Solvent accessible Surface area (A^2)	Molar refractivity (A^3)	Polarizability (A^3)	Log P	Theoretical IC_{50} (μM)	Synthetic accessibility
Boceprevir (ref)	550.05	532.13	485.254	133.615	34.535	0.736	8.0 ± 1.5	4.79
Boceprevir (cal)	550.10	533.01	485.314	133.710	34.487	0.744	8.5 ± 1.5	4.88
1	712.35	758.69	687.542	188.697	49.874	1.713	8.9 ± 1.5	4.98
2	735.55	715.31	657.998	195.568	52.287	1.845	8.8 ± 1.5	5.11
3	736.98	736.24	697.247	190.667	50.587	1.487	8.7 ± 1.5	4.90

QSAR/pharmacological descriptor analysis

The study is followed by the estimation of pharmacological descriptors for boceprevir and reported hit compounds. The values for the same are given in Table 3.

The calculated pharmacological properties include area of surface, volume, SASA, molar refractivity, polarizability, log P, theoretical IC_{50}, and synthetic accessibility. The area of surface and volume of the reported hit compounds are more than boceprevir. Solvent accessible surface area is the molecular area which is approachable (accessible) to any solvent. With respect to the surface and volume values, SASA of the reported compounds ranges from 697.247 to 697.247 A^2 which is higher than that of boceprevir. The molar refractivity depends on the volume of the molecule. The polarizability is a quantity to measure the contortion of the molecule under the influence of any field. The polarizability directly depends upon the dipole moment. Polarizability of the compounds ranges from 49.874 to 52.287 A^3. The value for the surface, volume, SASA, molar refractivity, and polarizability suggest that reported hit compounds are highly reactive to the surrounding medium as compared to boceprevir. In Table 3, log P is the measure of lipophilicity of the molecule calculated by taking the log of the partition coefficient. That is, the lipophilicity is inversely proportional to the value of log P. The calculated value of log P for reported hit compounds is more than boceprevir which indicates that the reported compounds are more hydrophilic, and therefore, they are more soluble in the biological environment of the body as compared to boceprevir. IC50 value of drugs is known as the half maximum inhibitory concentration measures substance's ability to inhibit a certain biological or metabolic activity. This empirical metric reflects in what quantity certain medicine and other such compound are required to suppress a physiological process by 50%. In vitro and in vivo experiments, it is widely employed as a criterion of adversary therapeutic potential. Synthetic accessibility term refers to the phenomena of fabrication of therapeutic compounds using easier and cheaper methods. Many sectors of the pharmaceutical industry require a methodology to determine the feasibility of fabrication (synthetic accessibility) of drug-like compounds. The creation and verification of a system capable of characterizing chemical synthetic accessibility score ranges from 1 (easier to synthesize) to 10 (complicated to develop) [24–26]. Collectively Table 2

and Table 3 are known as QSAR descriptors since they suggest the activity of the compounds based on their structure.

Table 4 Vibrational frequency analysis and comparison of boceprevir and reported virtual compounds

S. no	Normal distribution of vibrational mode	Experimental boceprevir (IR spectra in cm^{-1})	Theoretical boceprevir Using DFT/B3LYP/6-311G** (IR spectra in cm^{-1})	Hit compound 1 (IR spectra in cm^{-1})	Hit compound 2 (IR spectra in cm^{-1})	Hit compound 3 (IR spectra in cm^{-1})
1.	240 vibrational modes	3610	3556	3681	3632	3674
2.		3310	3249	3580	3566	3599
3.		3217	3167	3279	3268	3256
4.		3179	3119	3106	3119	3135
5.		3099	3068	3035	3012	3083
6.		3012	3045	2998	2883	2912
7.		1910	1803	2001	1993	2012
8.		1791	1709	1778	1697	1723
9.		1631	1566	1578	1597	1601
10.		1599	1537	1532	1547	1577
11.		1551	1521	1522	1515	1567
12.		1502	1451	1478	1423	1445
13.		1497	1340	1344	1340	1357
14.		1366	1277	1213	1251	1273
15.		1210	1206	1152	1112	1179
16.		1117	1103	1043	1001	1037
17.		1090	1041	1022	1078	1012
18.		960	961	945	952	927
19.		857	821	882	862	877
20.		799	718	785	763	772
21.		678	623	688	651	660
22.		570	565	567	550	512
23.		490	437	483	455	414
24.		375	325	315	325	360
25.		290	222	205	221	248

Spectroscopic analysis

To understand whether the geometry optimization took place in the transition state or the minimum state, vibrational transitions of the system were studied. Table 4 shows the vibrational analysis and comparison between boceprevir and reported hit compounds' structures using B3LYP/6-311G** and Fig. 1 shows the IR spectra of the reported molecules.

The computational infrared spectra of boceprevir hold a good agreement to that of experimental IR spectra results of boceprevir. The mean deviation between them is computed to be 74 cm^{-1}. To further understand the geometrical conformation of the reported hit structure, the independent mean deviation for compound 1, compound 2, and compound 3 is 21 cm^{-1}. The conversion of boceprevir to hit compounds remains localized in the entire system. No frequency was reported below 0 cm^{-1}; hence, the reported molecular structure will exist if designed synthetically. It is observed that OH bond stretching lies above 3012 cm^{-1}; the NH2 bending is observed within 1599–1502 cm^{-1}; C = O and C-O stretches are within 1497–1210 cm^{-1} and 1117–1090 cm^{-1}, respectively; also the N–C bends are within 1791–1631 cm^{-1}.

Molecular docking

After the optimization, the hit compounds were subjected to molecular docking. Molecular docking is a molecular engineering simulation skill that enables the interactions of two or more components in order to achieve a viable hybrid. Docking anticipates the three-dimensional configuration of the ligand-target complex based on the interacting affinities of the compound and the macromolecule. Using the aggregate of the energies, the docking calculations show the ideal lodged isoforms. Lead optimization, which indicates an optimum alignment of the ligand with its macromolecule, is one use of molecular docking; apart from the identification of hits. The binding affinities obtained after docking simulation are

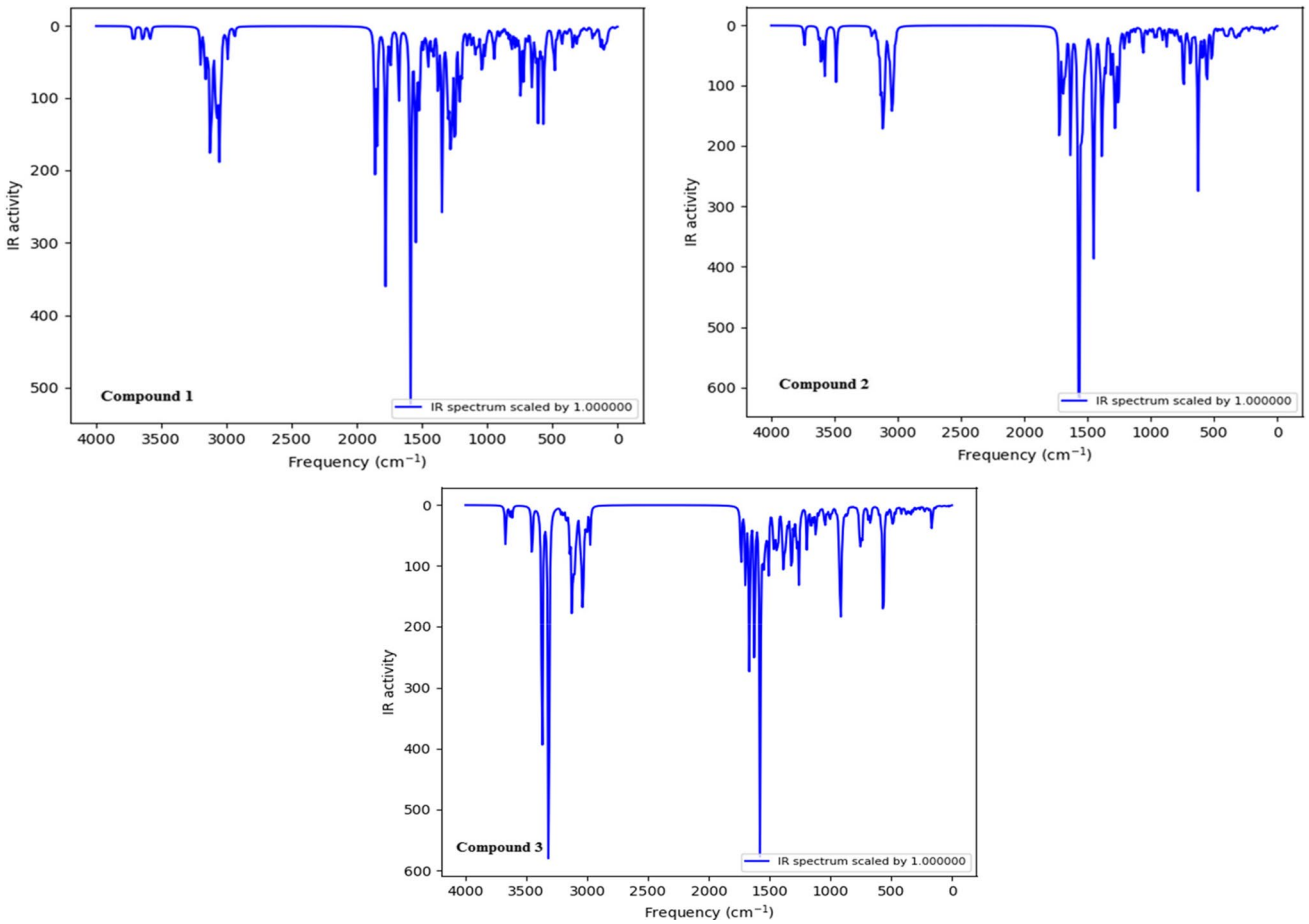

Fig. 1 IR spectra of the reported hit molecules

Table 5 Docking results of reported compounds with PDB ID: 7C6S

Compound	Binding affinity (kcal/mol)
1	−9.7
2	−8.5
3	−9.6
Boceprevir	−4.7

shown in Table 5. The comparative binding affinity of boceprevir was done by formulating the same parameters; the obtained results are given in the same table listed below. All three reported compounds show good binding affinity with the selected target.

Therefore, the characterized behavior of hit compounds with the opted targeted protein sites suggested that virtually designed molecules are capable of not only interacting with the macromolecule but also their interactions have good binding scores, thus ensuring the prophylaxis against COVID-19. Figure 2 shows the 2D interaction of the compounds with PDB ID: 7C6S in respective orders. The binding affinity of boceprevir with PDB ID: 7C6S is −4.7 kcal/mol. This indicates that reported compounds have greater binding affinity as compared to the boceprevir. In this figure, pink residues and interaction show alkyl interactions of the compound with the residues of the main chain. The green highlights and interaction show the hydrogen bonds formed by the compounds with the main chain. The Van der Waals interactions are represented by light green color.

Molecular dynamics

YASARA version 19.12.14.W.64 was used as computational simulation for carrying out molecular dynamics to understand the physical movement for 10 ns with 101 snapshots applying AMBER14 force field [21, 22]. MD simulation provided the structural integrity and changes in the conformations while the molecule is docked with the protein structure. Following parameters were set for carrying out the simulation: temperature at 298 K, pressure at bar, Coulomb electrostatic at 7.86 cutoff, and 2-fs time steps of periodic boundaries in one simulation box. Also, SPCE water model was used for carrying out MD simulations. Root mean square deviation (RMSD) and root mean square fluctuation

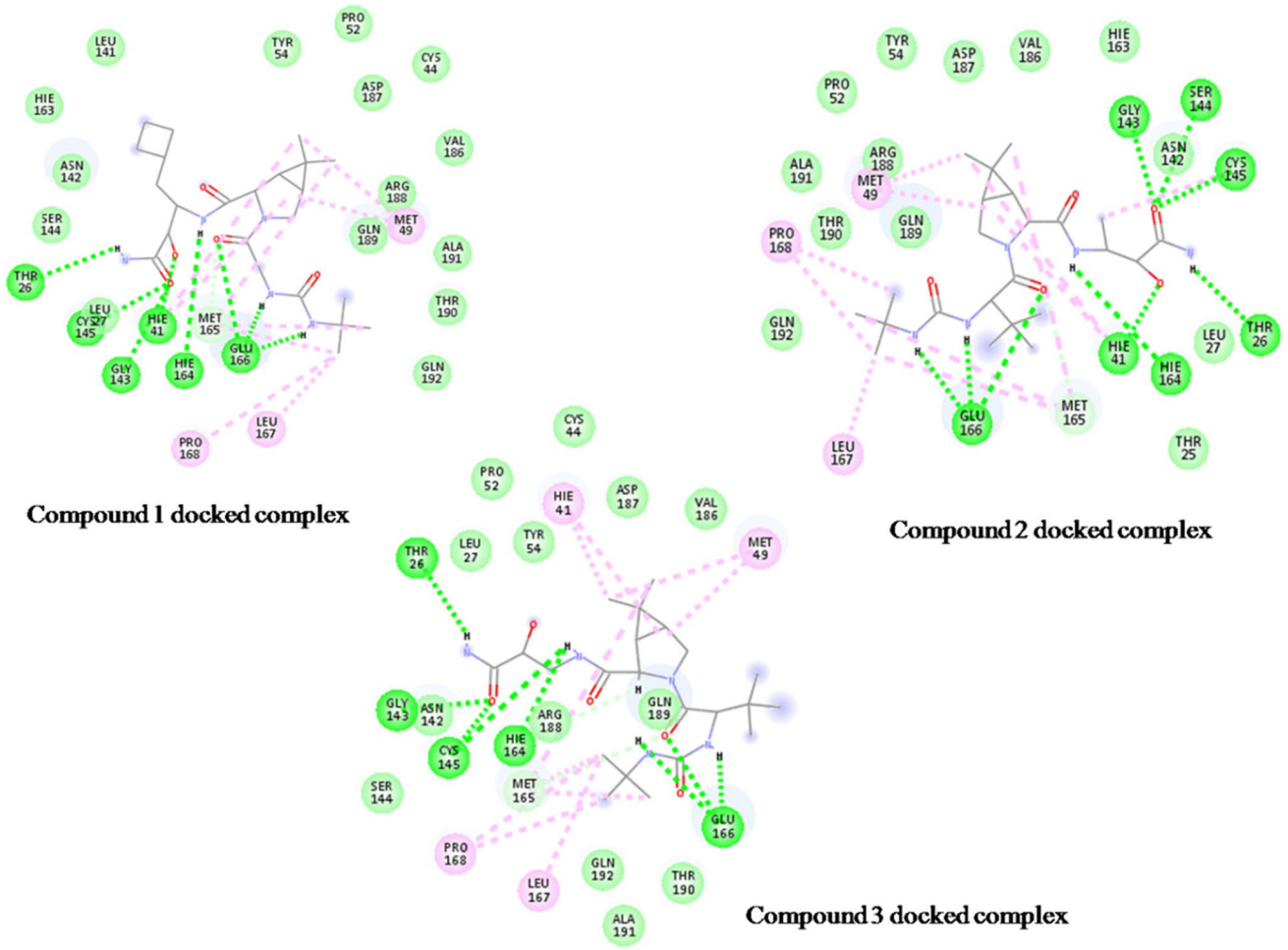

Fig. 2 2D interaction of the reported compounds with SARS-CoV-2 main protease. Here, pink, green, and light green residues and interactions represent the alkyl interactions, hydrogen bonds, and Van der Waals interactions, respectively

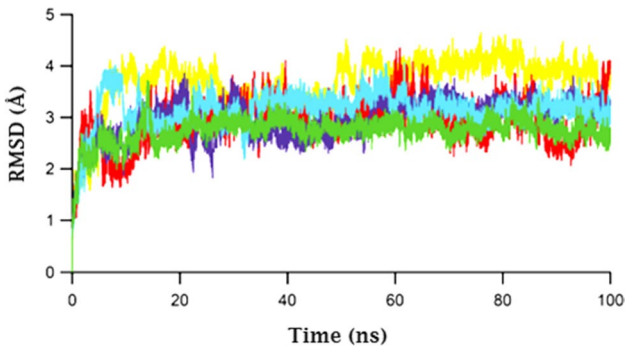

Fig. 3 RMSD of docked complexes. Here, yellow, red, blue, purple, and green represent compound 1, compound 2, compound 3, boceprevir, and protein backbone, respectively

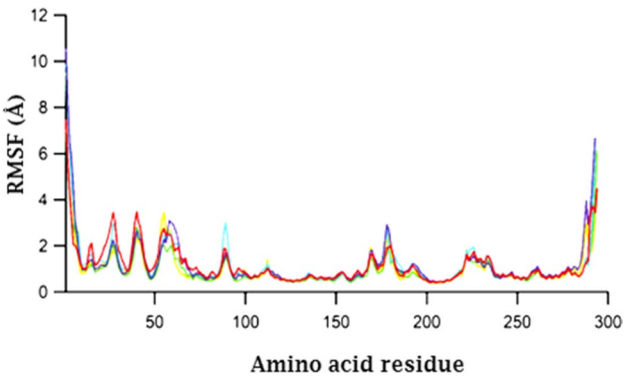

Fig. 4 RMSF plot of each amino acid. Here, yellow, red, blue, purple, and green represent compound 1, compound 2, compound 3, boceprevir, and protein backbone, respectively

(RMSF) assessments were used to examine conformational changes in the order to set stability of docked complexes. The graphical representations are given in Fig. 3 and Fig. 4. Here, in Fig. 3, yellow is compound 1, red is compound 2, blue is compound 3, purple is boceprevir, and green is the protein backbone; and in Fig. 4, yellow is compound

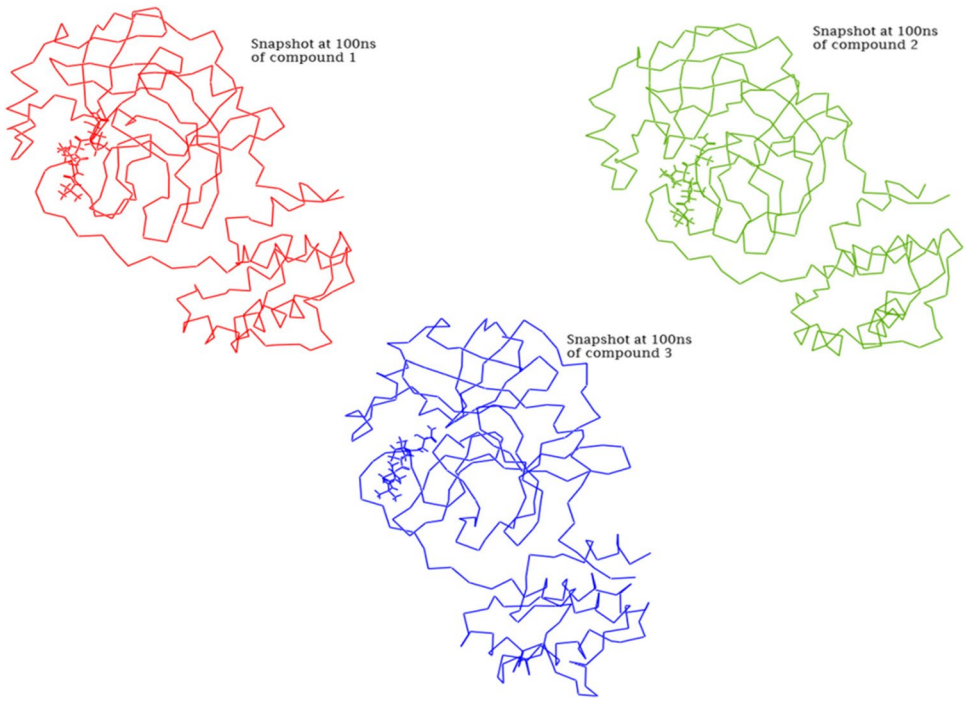

Fig. 5 The binding mode (3D) of each complex taken from final MD snapshot. Here, red, green, and blue represents snapshots for compound 1, compound 2, and compound 3, respectively

Table 6 Tabular representation for the results of MM-PBSA

MM-PBSA parameters	Compound 1	Compound 2	Compound 3	Boceprevir
Van der Waals energy	−241.61 ± 24.74	−242.62 ± 23.74	−243.63 ± 25.74	−224.76 ± 20.44
Electrostatic energy	−52.76 ± 8.21	−54.74 ± 8.11	−53.72 ± 10.11	−72.18 ± 12.46
Polar solvation	151.30 ± 7.87	155.33 ± 8.87	152.34 ± 5.88	246.27 ± 51.42
SASA	−22.39 ± 1.32	−25.41 ± 0.32	−26.40 ± 0.32	−26.04 ± 43.33
Binding energy	−165.46 ± 27.40	−166.40 ± 29.30	−164.49 ± 30.31	−74.71 ± 24.81

1, red is compound 2, blue is compound 3, and purple is boceprevir. The binding mode (3D) of each complex taken from final MD snapshot is also shown in Fig. 5. In this figure, red docked structure illustrates snapshot of PDB ID: 7C6S with compound 1, green illustrates snapshot of PDB ID: 7C6S with compound 2, and blue illustrates snapshot of PDB ID: 7C6S with compound 3.

The RMSD calculations revealed that three reported compounds were stable after 3 ns exhibiting deviations within the range of 1.5–4.23 A starting from 0.5 A for the reported complexes. The total binding energy of the three compounds was yielding more stable energy values. Each complex themselves exhibited deviations of approximately 0.5 A This resulted that docked complexes with each reported hit compounds resulted small deviations which signify that the complexes are stable within 100-ns time steps. The RMSF is an averaged measure of the displacement of a specific atom, or group of atoms, with respect to the reference structure. The analysis of the structure's time-dependent motions can benefit from the RMSD. The average variation of a particle (such as a peptide residue)

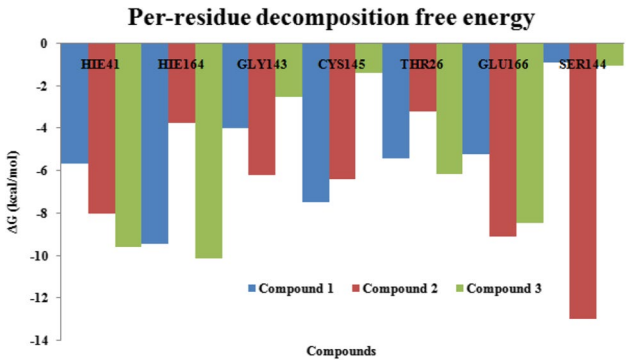

Fig. 6 Per-residue decomposition free energy of each docked complexes

upon time across a reference is measured by the RMSF. As a result, RMSF examines the structural aspects that deviates the most from their mean frame.

For understanding effects of interaction of ligand with main protease enzyme $3CL^{pro}$, average RMSF of protein constituting residues atoms resulted in minor fluctuations

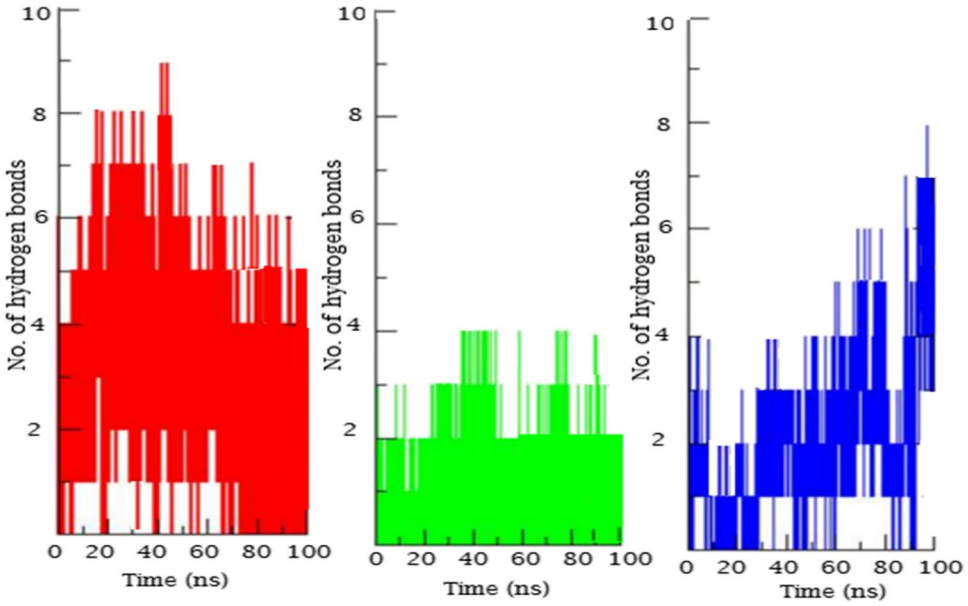

Fig. 7 Hydrogen bond analysis for the docked complex with the reported compounds. Here, red, green, and blue represent hydrogen bonds for complexes of compound 1, compound 2, and compound 3, respectively

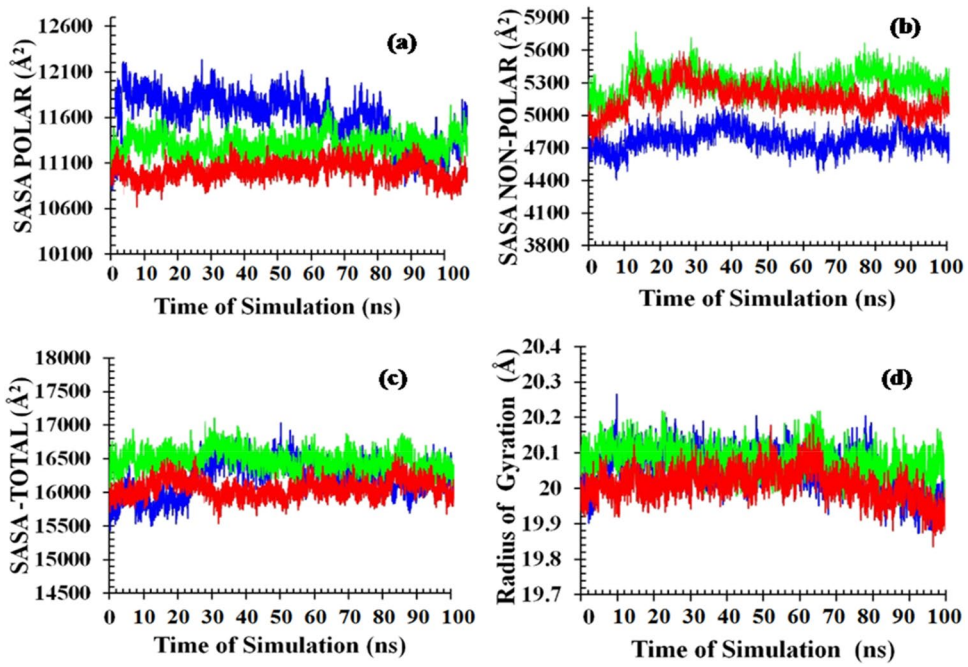

Fig. 8 Solvent accessible surface area (SASA) for 100-ns simulation at 300 K temperature. **a** SASA polar, **b** SASA non-polar, **c** SASA total, and **d** radius of gyration. Here, blue, green, and red represent compound 1, compound 2, and compound 3, respectively

between1.0 and 2.0 A. This MD simulation analysis resulted in prominent binding stability of drug compounds with PDB ID: 7C6S. The MM-PBSA calculations resulted as given in Table 6. Additionally, a per-residue graph of energy decomposition is illustrated in Fig. 6. It can be seen that HIE41 majorly favors the energy decomposition in each compound. Also, it can be seen that SER144 favors the energy decomposition only in compound 2. This shows that designed hit compounds have better binding strength as compared to boceprevir. Therefore, this signifies the ability to behave as stable compounds than the approved drug.

Hydrogen bond analysis is given in Fig. 7, analysis shown in red represents docked complex with compound 1, green represents docked complex with compound 2, and blue represents docked complex with compound 3. It was observed that the number of hydrogen bonds in the interaction of compound 1 are 9, for compound 2 number of hydrogen bonds are reported to be 4, whereas in compound 3, 8 hydrogen bonds were observed. This analysis was validated by the output obtained by the molecular docking studies.

The components of solvent accessible surface area (SASA) and radius of gyration (RoG) are shown in Fig. 8.

Table 7 Computed drug-like characteristics of the designed compounds

Properties	Compound 1	Compound 2	Compound 3
Human intestinal absorption	0.8765	0.9477	0.9041
Human oral bioavailability	0.5114	0.5120	0.5975
$CaCO_2$ permeability	0.5134	0.5424	0.5578
Blood–brain barrier	0.8799	0.9637	0.9119
p-Glycoprotein Inhibitor	0.5321	0.5215	0.5946
p-Glycoprotein Substrate	0.7597	0.7663	0.7390
CYP behavior	−0.5108	−0.5679	−0.5349
Acute oral toxicity	3.8671	2.4175	2.4668
Fish aquatic toxicity	0.4670	0.9496	0.8879

In this calculation, water was taken as the solvent for all the docked compounds. Here, blue represents compound 1, green represents compound 2, and red represents compound 3. In this, Fig. 8a shows SASA polar; it can be observed that compound 2 and compound 3 are constant throughout the 100-ns simulation. All the three reported compounds were stabilized after 3 ns until the final steps of MD simulation. Figure 8b shows the SASA non-polar, similar to the graph of SASA polar; it was observed that the reported compounds were stabilized after 3 ns and they remained stable throughout the simulations. Figure 8c shows the total SASA of the reported compounds; each docked complex was stable during the 100-ns simulation when water was used as the solvent, and this shows that these molecules possess a tendency to maintain their stability with water as the solvent.

Figure 8d shows the radius of gyration of the reported hit compounds. RoG illustrates the compact nature of the protein backbone when made to interact with the water solvent. The stable curves of each compounds shows that the reported compounds are compact and rigid in nature, thus the interactions of the reported compounds are stable with receptor (PDB ID: 7C6S).

ADMET analysis

To understand the metabolic behavior of the reported compounds, ADMET analysis was done. The observed parameters are listed in Table 7.

Conclusion

The reported hit compounds of boceprevir designed via fragment-based drug designing have improved electronic, thermodynamical, and pharmacological properties as compared to FDA-approved boceprevir. In context with total energy, ΔE value, dipole moment, and heat of formation all three hit compounds are more stable and reactive, and theoretical IC_{50} value estimation resulted that these molecules will be required in smaller doses to achieve successful and long lasting results. The docking studies of these compounds with PDB ID: 7C6S, PDB ID: 6LZG, and PDB ID: 7NX7 suggested that they exhibit greater binding affinity as compared to boceprevir. The RMSD calculations revealed that the three reported compounds were stable after 3 ns showing RMSD calculations within range of 1.5–4.23 A starting from 0.5 A . Also, the results of hydrogen bond analysis validated the results of docking simulation. Therefore, these reported compounds can be designed in laboratory followed by their clinical trials. The designed compounds exhibited a greater affinity than the original chemical, according to the MM-PBSA binding energy study, making it a promising option for more drug development research.

Acknowledgements Prashasti Sinha is very thankful to the University Grant Commission (UGC), New Delhi, India, for the financial support for doctoral research work. The authors would like to acknowledge IIT Delhi, India, for allowing the access of SCFBio web server.

Author contribution P. Sinha and A.K. Yadav have contributed equally in the work.

Data Availability All the relevant data has been given in the article.

Declarations

Competing interests The authors declare no competing interests.

References

1. Mahato S (2022) Med Chem18: 847
2. Narayanan A, Toner SA, Jose J (2022) Biochem Soc Trans 50:151
3. Kneller D, Li H, Phillips G, Weiss K, Zhang Q, Arnould M, Kovalevsky A (2022) Nat Commun 13:1
4. Akbulut E (2022) Braz Archives Biol Technol. 64: e21200803
5. Kumar P, Mohanty D (2021) Mol Inform 41:2100178
6. Premkumar L, Segovia-Chumbez B, Jadi R, Martinez DR, Raut R, Markmann A, de Silva AM (2020) Sci Immunol 5:1
7. Anthony SJ, Johnson CK, Greig DJ, Kramer S, Che X, Wells H, Goldstein T (2017) Virus Evol 3:1
8. Padhi AK, Tripathi T (2020) ACS Pharmacol Trans Sci 3:1023
9. Gasmi A, Mujawdiya PK, Lysiuk R, Shanaida M, Peana M, Benahmed AG, Bjørklund G (2022) Pharmaceuticals 15:1049
10. Zhu J, Zhang H, Lin Q, Lyu J, Lu L, Chen H, Chen K (2022) Drug Design Development aTherapy 16:1067
11. Alai S, NGujar M, Joshi M, Gautam S (2021) Gairola Heliyon. 7: e06564
12. Fu L, Ye F, Feng Y, Yu F, Wang Q, Wu Y, Gao GF (2020) Nat Commun 11:1
13. Dejnirattisai W, Zhou D, Supasa P, Liu C, Mentzer AJ, Ginn HM (2021) GRScreaton Cell 184:2939
14 Hao GF, Jiang W, Ye YN, Wu FX, Zhu XL, Guo FB (2016) Nucleic Acids Res 44:W550
15. Frisch MJ, Trucks GW, Schlegel HB (2009) Gaussian 09.(Gaussian Inc, Wallingford) (Revision D.01)
16. Becke AD (1993) J Chem Phys 98: 5648

17 Lee C, Yang W, Parr RG (1988) Phys Rev B 37:785
18 Morris GM, Huey R, Lindstrom W, Sanner MF, Belew RK, Goodsell DS, Olson AJ (2009) J Comput Chem 30:2785
19 Saleh NA, Ezat AA, Elfiky AA, Elshemey WM, Ibrahim M (2015) J Comput Theoretical Nanosci 12:371
20. Ezat AA, Elfiky AA, Elshemey WM, Saleh NA (2019) Virus Dis 30:207
21 Land H, Humble MS (2018) Protein Eng 1685:43
22 Bhadra P, Siu SW (2019) Langmuir 35:9622
23 Kumari R, Kumar R (2014) J Chem Inf Model 54:1951
24 Sinha P, Yadav AK (2022) J Comput Biophys Chem 21:783
25. Sinha P, Yadav AK (2022) Comput Theoretical Chem 1217:113919
26. Sinha P, Yadav AK (2023) J Biomol Struct Dynamics